

## Momentum-Space Entanglement Spectrum of Bosons and Fermions with Interactions

Rex Lundgren,<sup>1,\*</sup> Jonathan Blair,<sup>1</sup> Martin Greiter,<sup>2</sup> Andreas Läuchli,<sup>3</sup> Gregory A. Fiete,<sup>1</sup> and Ronny Thomale<sup>2</sup>

<sup>1</sup>*Department of Physics, The University of Texas at Austin, Austin, Texas 78712, USA*

<sup>2</sup>*Institute for Theoretical Physics, University of Würzburg, D-97074 Würzburg, Germany*

<sup>3</sup>*Institut für Theoretische Physik, Universität Innsbruck, Technikerstraße 25, A-6020 Innsbruck, Austria*

(Received 13 May 2014; published 18 December 2014)

We study the momentum space entanglement spectra of bosonic and fermionic formulations of the spin-1/2 XXZ chain with analytical methods and exact diagonalization. We investigate the behavior of the entanglement gaps, present in both formulations, across quantum phase transitions in the XXZ chain. In both cases, finite size scaling suggests that the entanglement gap closure does not occur at the physical transition points. For bosons, we find that the entanglement gap observed in Thomale *et al.* [Phys. Rev. Lett. 105, 116805 (2010)] depends on the scaling dimension of the conformal field theory as varied by the XXZ anisotropy. For fermions, the infinite entanglement gap present at the XX point persists well past the phase transition at the Heisenberg point. We elaborate on how these shifted transition points in the entanglement spectra may support the numerical study of phase transitions in the momentum space density matrix renormalization group.

DOI: [10.1103/PhysRevLett.113.256404](https://doi.org/10.1103/PhysRevLett.113.256404)

PACS numbers: 71.10.Pm, 03.67.Mn, 11.25.Hf

*Introduction.*—Quantum information ideas applied to condensed matter systems have revealed novel insights into exotic phases of matter [1]. Quantitatively, quantum information between two regions,  $A$  and  $B$ , can be characterized by the ground state reduced density matrix of  $A$ ,  $\rho_A$  and analogously  $B$ ,  $\rho_B$ . For example, the entanglement entropy (EE) is given by  $\text{Tr}(\rho_A \ln \rho_A) = \text{Tr}(\rho_B \ln \rho_B)$ . The entanglement spectrum (ES) [2] (defined as the set of eigenvalues of a fictitious entanglement Hamiltonian,  $H_e$ , with  $\rho_A$  written as  $e^{-H_e}$ ) is a useful tool in understanding topological states of matter and strongly correlated systems, including fractional quantum Hall (FQH) systems [2–10], quantum spin chains [11–17] and ladders [18–26], topological insulators [27–32], symmetry broken phases [33,34], and other systems in one [35–39] and two [40–52] spatial dimensions. These studies predominantly focused on real or orbital space entanglement. For many gapped systems, the energy spectrum of the edge states and ES are equivalent. This was proven by X. L. Qi *et al.* [53] and elaborated on in Refs. [23,54–56]. There is no universal understanding of systems with a gapless bulk, where long range correlations are present [57].

The ES in momentum space has been explored in quantum spin chains [11] and ladders [20]. A momentum partition is natural and physically relevant, as the low-energy formulation of one-dimensional systems involves the splitting of particles into left and right movers [58]. A deeper understanding of the momentum space ES could help identify the most fruitful applications of momentum space density matrix renormalization group (DMRG) algorithms [59–62]. Gapless spin chains are one promising candidate for the momentum space DMRG. For example, for chains with higher symmetry groups, characterizing the

parameters of the critical theories is a challenge for the real space DMRG and motivates different formulations [63]. The momentum space ES is also useful in characterizing disordered fermionic systems [64–66] as well as in quantum field theories, where large momenta are traced over [67].

The momentum space ES of the spin-1/2 Heisenberg model exhibits a fingerprint of the underlying conformal field theory (CFT) in the counting of the entanglement levels and a large entanglement gap (EG), a notion first observed in the conformal limit construction of FQH entanglement spectra [3]: The counting of the entanglement levels below the EG in the spin chain relates the U(1) boson counting in the gapless sine-Gordon regime to the U(1) edge of the bosonic Laughlin state. The spin chain EG becomes infinite at the Haldane-Shastry (HS) [68,69] point, whose Fourier transformed wave function yields the same weights of monomials as the Laughlin state. This fits into a more general connection of certain critical quantum spin chains and FQH states [70,71].

As was recently pointed out, the ES may provide a useful indication of distinct phases, but not phase transitions [72,73]. In particular, Ref. [72] highlighted that phase transitions can occur in the real-space entanglement Hamiltonian even though the physical ground state remains the same. (Ref. [3] noted early on that transitions according to an EG closure appear shifted as compared to the physical system.) Physically, this is because the properties of a system are determined by  $H_e$  at finite temperature. Furthermore, Ref. [73] stressed that nonanalyticities of the ES can be connected to symmetries in real space, and are not always linked to phase transitions. In view of numerical techniques such as the DMRG, whose performance is directly tied to the ES, we wish to convey that the persistence of EGs

beyond physical transitions might improve the performance of DMRG algorithms. If the entanglement weight below the gap still provides an effective representation of entanglement contained in the state, the presence of an EG promises a reasonably constant performance of the numerical algorithm as one sweeps over the physical phase transition.

In this Letter, we explore the ES in momentum space for fermions and bosons in the  $XXZ$  spin-1/2 chain. We find, in both cases, the ES fails to capture features of physical phase transitions. For bosons, we find the EG seen by Thomale *et al.* [11] is not always observed for CFTs of the same central charge,  $c$ , but different scaling dimensions. We also find that the bosonic momentum space ES at the Heisenberg point is flat, and despite similarity to the FQH Laughlin state, lacks topological entanglement entropy (TEE) [74–76]. For fermions, we observe, from finite size scaling, that the EG does not capture the phase transition present in the  $XXZ$  spin-1/2 chain. We argue that due to their deviation from the physical phase transitions, the properties of the entanglement spectral flow might prove useful for entanglement-based numerical applications.

*Model and details of partition.*—We investigate the  $XXZ$  spin-1/2 chain, represented by hardcore bosons and by Jordan-Wigner fermions. The Hamiltonian with nearest and next-nearest neighbor interactions is given by

$$H = \sum_{n=1}^2 \sum_{i=1}^N J_n (S_i^x S_{i+n}^x + S_i^y S_{i+n}^y + \Delta S_i^z S_{i+n}^z), \quad (1)$$

with periodic boundary conditions (PBCs) and length  $N$ . The transformation from spin operators to bosons is given by  $S_i^+ = b_i^\dagger$ ,  $S_i^- = (b_i^\dagger b_i - \frac{1}{2})$ , with an added hard-core term that prevents double occupancy. The hard-core term is an important source of entanglement in momentum space for bosons [77] and leads to differences in the ES between bosonic and fermionic formulations. Most literature has focused on the similarity of physical properties of bosons and fermions in one dimension [79]; this Letter highlights a difference between bosons and fermions. The transformation to fermions is given by the Jordan-Wigner transform,  $S_i^+ = c_i^\dagger \prod_{j=1}^{i-1} (1 - 2c_j^\dagger c_j)$  and  $S_i^- = (c_i^\dagger c_i - \frac{1}{2})$ . The phase diagram of Eq. (1) is well studied [79,80]. We focus on the regime  $0 \leq \Delta < 3$  and  $J_2 = 0$  for the main part of the manuscript. For  $0 \leq \Delta \leq 1$ , the model is in a gapless phase with  $c = 1$ . The fermions are free at  $\Delta = 0$  and acquire interactions of increasing strength with increasing  $\Delta$ ; the bosons are strongly interacting throughout due to the hard-core term.  $\Delta = 1$  is the  $SU(2)$  symmetric Heisenberg point. For  $\Delta > 1$ , the model is in the gapped Ising phase. To set up a momentum space partition of the Hilbert space, we Fourier transform the bosons (fermions) as  $(b, c)_j = (1/\sqrt{N}) \sum_{m=-\frac{N}{2}+1}^{\frac{N}{2}} e^{imj} (b, c)_m$ , where  $m$  is the crystal momentum. Momentum basis states are labeled by occupation number,  $n_m$ , and crystal momentum,  $(2\pi m/N)$ ,  $m \in \{-\frac{N}{2}+1, \dots, \frac{N}{2}\}$ . The ground state of Eq. (1) has

$S_{\text{tot}}^z = \sum_{i=1}^N S_i^z = 0$  for the range of parameters we consider. Thus, the number of bosons and fermions,  $N_p$ , is  $N/2$ . For fermions, we consider system sizes of  $4n+2$ ,  $n \in \mathbb{N}$ , to avoid a degenerate Fermi sea at  $\Delta = 0$ .

After the ground state is obtained via exact diagonalization in the momentum occupation basis, we partition the system into two regions,  $A$  and  $B$ , by dividing the momentum occupation basis at  $\Gamma$ , i.e.,  $m \in A = \{m|m > 0\}$  and  $m \in B = \{m|m \leq 0\}$  and fixing the particle number in each region. We form the density matrix and then trace out the degrees of freedom of  $B$ . This yields  $\rho_A$  and  $H_e$ . The total momentum,  $M = \sum_m n_m m$ , is only conserved approximately, and maps to the exact quantum number of total crystal momentum via  $M_C = M \bmod N$ . Still, the total momentum can be a useful approximate quantum number when a large percentage of the weight is located in one sector as seen for the bosonic ground states near  $\Delta = 1$ . (At the HS point, the total bosonic momentum becomes an exact quantum number [11].) In such a case, we partition with respect to both number of particles and total momentum with the constraints  $N_A + N_B = N_p$  and  $M_A + M_B = M$ . For a wave function with strongly distributed weight in several momentum sectors (which happens for fermions), the total momentum is not a valid quantum number, and several momentum sectors will be mixed. In this case, we partition the system with respect to the number of particles and total crystal momentum of  $A$  and  $B$ , i.e.,  $M_{A,C} + M_{B,C} = M_C$ . One can visualize the momentum space cut as a tracing out one half of two coupled chiral one-dimensional systems. Because of the numerical limitations of exact diagonalization, we consider system sizes up to  $N = 22$  for bosons and  $N = 30$  for fermions.

*Revisiting the Heisenberg point.*—Reference [11] hinted that the ES for bosons below the EG is flat. We now show numerical evidence for this and analyze the consequences of a flat ES. We find the average of the levels at each  $M_A$  below the EG approach the same constant value in the

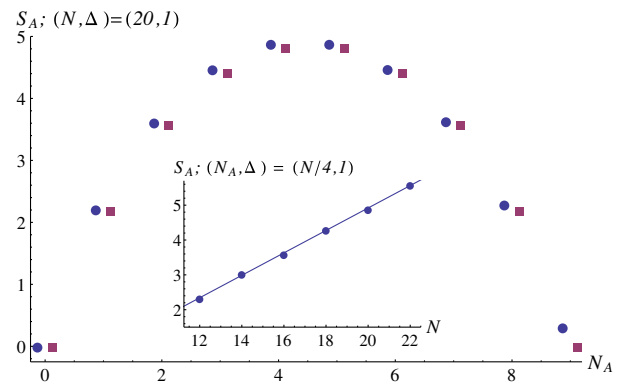


FIG. 1 (color online). EE of bosons,  $S_A$ , versus  $N_A$  at  $\Delta = 1$  for 20 sites (blue circle). EE assuming a flat ES (violet square). Inset:  $S_A(N/4)$  versus  $N$  ( $N_A = N/4 - 1/2$  if  $N/2$  is odd).  $S_A$  is fit well by a linear equation, as expected for large  $N$ .

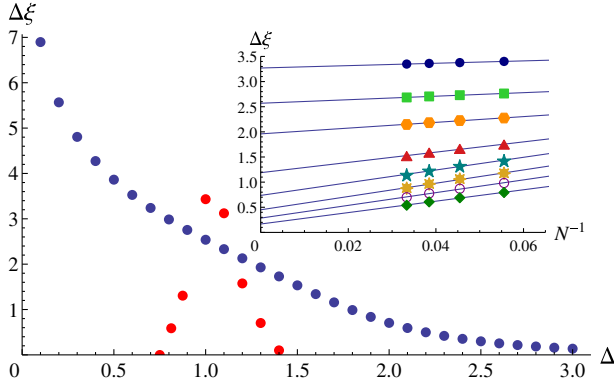


FIG. 2 (color online). The TD projection [from finite size scaling with  $N_A = N_p/2$  ( $N_A = \frac{N_p-1}{2}$  if  $N_p$  is odd)] of the EG,  $\Delta\xi$ , for fermions (blue circle) and bosons (red circle) versus  $\Delta$ . Inset: Finite size scaling of the EG for fermions versus  $\Delta$ . All data fit the form  $\Delta\xi = \alpha + \frac{\beta}{N}$ , where  $\alpha, \beta > 0$ . Parameters:  $\Delta = .7$  (navy blue disk),  $\Delta = 1$  (green square),  $\Delta = 1.3$  (orange hexagon),  $\Delta = 1.6$  (red triangle),  $\Delta = 2.0$  (teal star),  $\Delta = 2.3$  (yellow eight-point star),  $\Delta = 2.6$  (purple empty circle), and  $\Delta = 3.0$  (green diamond).

thermodynamic (TD) limit approximately equal to the natural log of the number of levels below the EG,  $N_g = [((N_p - 1)!)/((N_p - 1 - N_A)!(N_A)!)]$ . This numerically demonstrates that the ES is flat, so we can investigate how the EE scales with  $N$ . Neglecting the levels above the EG (this approximation is exact at the HS point), the normalization condition for the trace of  $\rho_A$  is set to  $1 = \sum_{i=1}^{N_g} e^{-\xi_i} = N_g e^{-\xi}$ , where  $\xi_i$  are the entanglement eigenvalues. The EE is then  $S(N_A) = \ln(N_g)$ . In the large  $N_p$  limit, we obtain a linear, i.e., volume scaling for the EE, different from the standard area law seen in real space systems [81]. (This volume scaling hints at a drawback of the momentum space DMRG from the view of general information theory. Still, the structure of the ES might render this formulation advantageous in the end, for the range of finite system sizes which are available.) By varying  $N_A$  and expanding the EE in the large  $N_p$

limit around  $N_A = (N_p/2)$ , we find  $S_A(N_p, N_A) = S_A(N_A = (N_p/2)) - (2/N_p)((N_p/2) - N_A)^2$ . This behavior at  $\Delta = 1$  is shown in Fig. 1.

Despite a similarity in state counting to the Laughlin ES on the quantum Hall sphere, one important difference is that the ES at the Heisenberg point is flat, consistent with the Heisenberg point being nonchiral. (Note the ES of the FQH Laughlin state on the sphere mimics a linearly dispersing chiral  $U(1)$  mode in the conformal limit [3].) An important consequence of the flat spectrum at the Heisenberg point is the absence of TEE, which we confirmed numerically, whereas the FQH Laughlin state on the sphere exhibits TEE [76].

*Bosonic entanglement gap.*—We now vary  $\Delta$  and investigate the behavior of the EG (Fig. 2). Adjusting  $\Delta$  varies the scaling dimension of the underlying CFT in the gapless phase. As stated before, the EG is infinite at the HS point (which can be thought of as an  $SU(2)$  invariant deformation away from the Heisenberg point), at which the fractionalized excitations, spinons, are free and interact only through their mutual statistics. Moving from the HS point to the Heisenberg point introduces interactions between spinons and dresses the state, but the EG still persists in the TD limit. The EG for bosons is defined as the minimal difference between the generic entanglement levels and the low lying universal levels. Our conclusions do not depend on whether we define the EG as a direct gap constrained to a given sector ( $N_A, M_A$ ) or as a global gap over all  $M_A$ . We find that the EG for bosons is not open throughout the entire gapless region. This is not affected by either considering an approximate decomposition in total momentum or an exact decomposition in crystal momentum.

Figure 3 shows representative plots of the bosonic ES as a function of  $\Delta$ . The EG decreases as  $\Delta$  is lowered from 1. Qualitatively, this is due to interactions developing between spinons, which further dress the approximate productlike spinon state present at the Heisenberg point. The EG for 22 sites closes at  $\Delta \approx \frac{1}{4}$ . Finite size scaling reveals that, in the TD limit, the EG closes at  $\Delta \approx \frac{3}{4}$  (Fig. 2). The exact location of the closure is beyond the scope of this Letter. Rather, the important feature is the closure of the EG for some value

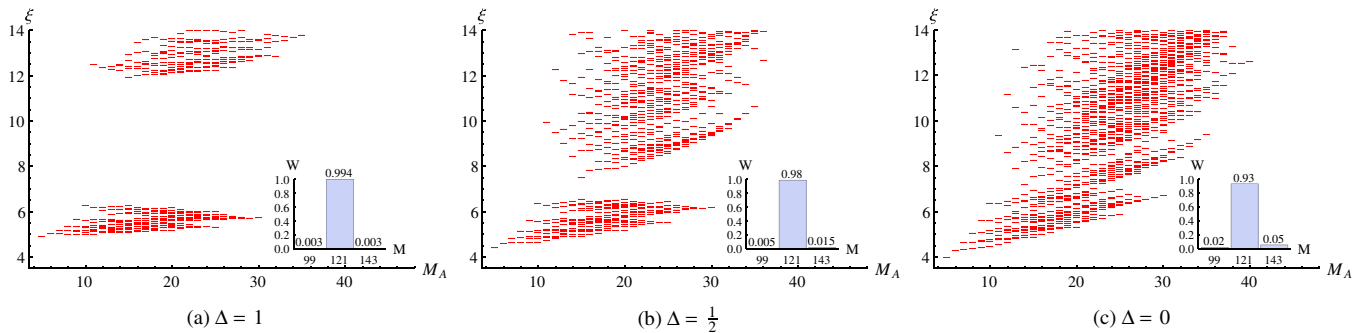


FIG. 3 (color online). Bosonic ES for representative values of  $\Delta$ , with  $N = 22$  and  $N_A = 5$ . The entanglement eigenvalues  $\xi$  are plotted versus  $M_A$ . Inset: Fraction of weight of the ground state,  $W$ , versus  $M$ . The ground state primarily resides in the  $M = N^2/4$  sector.

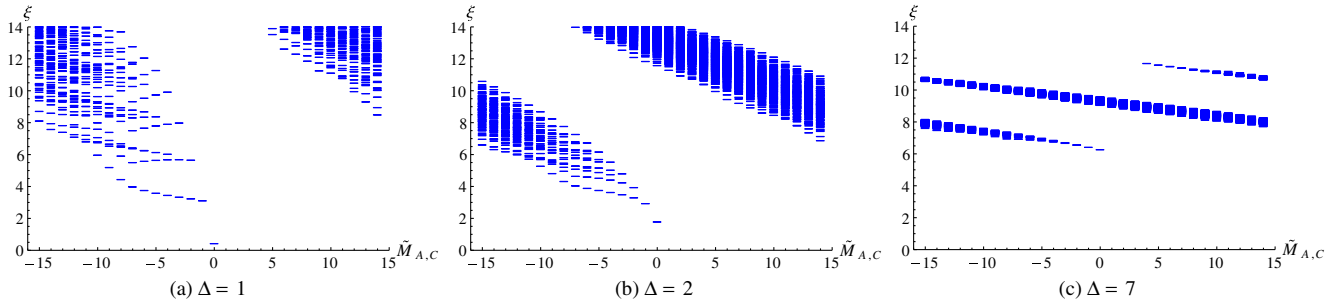


FIG. 4 (color online). Fermionic ES for representative values of  $\Delta$ , with  $N = 30$  and  $N_A = 7$ . The fermionic ES remains qualitatively similar for  $\Delta = 1$  and  $\Delta = 2$  despite a phase transition at  $\Delta = 1$  and is linear for  $\Delta = 7$ . The entanglement eigenvalues  $\xi$  are plotted versus  $\tilde{M}_{A,C} = M_{A,C} + 13$ . We have shifted the Brillouin zone by  $M_C = 13$  to have the lowest level at  $\tilde{M}_{A,C} = 0$ .

of  $\Delta$  in the gapless regime. This is seen even for finite system sizes. It might allow for the interpretation that the momentum space EG is not, by itself, a necessary signature for a gapless  $S = 1/2$  spin fluid state.

Note real space symmetries also yield fingerprints in the momentum space ES for bosons. For  $\Delta = 0$ , one can unitarily transform the Hamiltonian from negative  $J_1$  to positive  $J_1$  by a  $\pi$  rotation about the  $z$  axis on every second site. We analytically show in the Supplemental Material [77] that this leads to a shift in momentum by half a lattice vector and a reflection in the ES. We also prove a reflection seen in the bosonic ES for  $J_1 = 0, J_2 \neq 0$ .

*Fermionic ES.*—Figure 4 shows plots of the fermionic ES for representative values of  $\Delta$ . We first observe that the counting of  $1, 1, 2, 3, 5, \dots$  for all values of  $\Delta$  (Fig. 4), starting from  $\tilde{M}_{A,C} = 0$ , is trivial, as it links to total Hilbert space state counting in the respective momentum sector. This highlights the importance of the  $U(1)$  counting seen for bosons near  $\Delta = 1$  where the Hilbert space is not exhausted by this counting.

At  $\Delta = 0$ , the fermionic left and right movers are not entangled and form a product state [82,83] with an infinite EG. Qualitatively, the gap decreases as we increase  $\Delta$  from zero due to interactions developing between fermions, complementary to what is observed for bosons. The EG captures the low energy properties of  $H_e$ , thus, phase transitions in  $H_e$ . Figure 2 shows the TD projection of the fermionic EG. The EG remains relatively large and finite well past  $\Delta = 1$ . The inset of Fig. 2 shows that the scaling with inverse system size always decays linearly and the gap remains open in the TD limit past  $\Delta = 1$ . For  $\Delta \gtrsim 1.7$ , the system sizes we consider are larger than the correlation length [84], so we expect our scaling to be reliable. For example, the correlation length for the charge stiffness, taken from Ref. [84], is  $\approx 1.5$  lattice spacings for  $\Delta = 3$ , while the largest system size we consider is 10 times bigger (dividing  $N$  by two due to PBCs). This should also be compared to the scaling difference between the two lowest physical energy levels. Analyzing the scaling of the difference in the two lowest physical energy levels in the XXZ model, one can accurately detect the phase transition at

$\Delta = 1$  with only ten sites [85]. As such, the system sizes considered here are large enough in principle to detect phase transitions near the TD value. We conclude that the EG and the ES systematically do not capture the phase transition from the gapless to gapped phase.

The ES deep in the Ising phase is linear as seen in Fig. 4(c) [77]. This adds to the argument that the EG extends past  $\Delta = 1$ . The reasoning is as follows: Starting near the transition (on the gapped side) of  $H_e$  (at zero entanglement temperature,  $T_e$ ) we can imagine increasing  $T_e$ . Increasing  $T_e$ , we expect the gapped phase to become gapless due to thermal fluctuations, thus, giving us the required physical phase diagram at  $T_e = 1$  [72].

*Conclusions.*—We have studied the momentum space ES for both bosons and fermions. We have shown with analytical methods and exact diagonalization, that the momentum space ES fails to detect physical phase transitions. More explicitly, the EG seen for bosons [11] does not remain open for arbitrary scaling dimensions in the  $c = 1$  CFT domain. For fermions, we found that the low energy (highly entangled) part of  $H_e$  does not host a phase transition near a corresponding physical phase transition. Our findings for fermions suggest that the results of Ref. [64], which state that momentum space ES can characterize disordered one-dimensional fermionic systems, need to be taken with caution in the presence of interactions.

Our results are useful for numerical techniques such as the DMRG, where one discards states of  $\rho_A$  with low entanglement. For both fermions and bosons, a large separation of scales in entanglement persists in a relatively large region around the phase transition at  $\Delta = 1$ . Assuming there is still enough entanglement weight located below the EG, this might, despite a volume law for EE, allow a momentum space based DMRG code to probe the critical point and the region around it. This work highlights that the nonuniversality of the ES pointed out in Ref. [72] might in certain cases establish a useful feature for numerical applications.

We thank V. Chua, S. Furukawa, M. Oshikawa, D. Lorschbough, and P. Laurell for useful discussions. R. T.



particularly thanks D. Arovass and B. A. Bernevig for discussions and collaborations on related topics. R. L. was supported by NSF Graduate Research Fellowship Grant No. 2012115499. R. L. acknowledges the hospitality of the Insitute for Theoretical Physics, Univesity of Würzburg, and University of Tokyo where part of this work was completed under NSF EAPSI Grant No. OISE-1309560 and Japan Society for the Promotion of Science (JSPS) Summer Program 2013. A. M. L. acknowledges support through Grant No. FOR1807 (DFG/FWF). G. A. F. acknowledges financial support through ARO Grant No. W911NF-09-1-0527 and NSF Grant No. DMR-0955778. M. G. and R. T. are supported by the ERC starting Grant TOPOLECTRICS of the European Research Council (ERC-StG-Thomale-2013-336012). The authors acknowledge the Texas Advanced Computing Center (TACC) at The University of Texas at Austin for providing computing resources that have contributed to the research results reported within this paper [86].

\*rexlund@physics.utexas.edu

- [1] L. Amico, R. Fazio, A. Osterloh, and V. Vedral, *Rev. Mod. Phys.* **80**, 517 (2008).
- [2] H. Li and F. D. M. Haldane, *Phys. Rev. Lett.* **101**, 010504 (2008).
- [3] R. Thomale, A. Sterdyniak, N. Regnault, and B. A. Bernevig, *Phys. Rev. Lett.* **104**, 180502 (2010).
- [4] R. Thomale, B. Estienne, N. Regnault, and B. A. Bernevig, *Phys. Rev. B* **84**, 045127 (2011).
- [5] A. M. Läuchli, E. J. Bergholtz, J. Suorsa, and M. Haque, *Phys. Rev. Lett.* **104**, 156404 (2010).
- [6] I. D. Rodriguez, S. C. Davenport, S. H. Simon, and J. K. Slingerland, *Phys. Rev. B* **88**, 155307 (2013).
- [7] I. D. Rodriguez, S. H. Simon, and J. K. Slingerland, *Phys. Rev. Lett.* **108**, 256806 (2012).
- [8] A. Sterdyniak, N. Regnault, and G. Möller, *Phys. Rev. B* **86**, 165314 (2012).
- [9] J. Dubail, N. Read, and E. H. Rezayi, *Phys. Rev. B* **85**, 115321 (2012).
- [10] T. S. Jackson, N. Read, and S. H. Simon, *Phys. Rev. B* **88**, 075313 (2013).
- [11] R. Thomale, D. P. Arovass, and B. A. Bernevig, *Phys. Rev. Lett.* **105**, 116805 (2010).
- [12] V. Alba, M. Haque, and A. M. Läuchli, *J. Stat. Mech.* **8**, 11 (2012).
- [13] F. Pollmann, A. M. Turner, E. Berg, and M. Oshikawa, *Phys. Rev. B* **81**, 064439 (2010).
- [14] G. De Chiara, L. Lepori, M. Lewenstein, and A. Sanpera, *Phys. Rev. Lett.* **109**, 237208 (2012).
- [15] M. S. Ramkarthik, V. R. Chandra, and A. Lakshminarayan, *Phys. Rev. A* **87**, 012302 (2013).
- [16] F. Franchini, A. Its, V. Korepin, and L. Takhtajan, *Quantum Inf. Process.* **10**, 325 (2011).
- [17] L. Lepori, G. De Chiara, and A. Sanpera, *Phys. Rev. B* **87**, 235107 (2013).
- [18] D. Poilblanc, *Phys. Rev. Lett.* **105**, 077202 (2010).
- [19] A. M. Läuchli and J. Schliemann, *Phys. Rev. B* **85**, 054403 (2012).
- [20] R. Lundgren, V. Chua, and G. A. Fiete, *Phys. Rev. B* **86**, 224422 (2012).
- [21] X. Chen and E. Fradkin, *J. Stat. Mech.* (2013) P08013.
- [22] J. I. Cirac, D. Poilblanc, N. Schuch, and F. Verstraete, *Phys. Rev. B* **83**, 245134 (2011).
- [23] R. Lundgren, Y. Fuji, S. Furukawa, and M. Oshikawa, *Phys. Rev. B* **88**, 245137 (2013).
- [24] S. Tanaka, R. Tamura, and H. Katsura, *Phys. Rev. A* **86**, 032326 (2012).
- [25] V. Alba, M. Haque, and A. M. Läuchli, *Phys. Rev. Lett.* **108**, 227201 (2012).
- [26] W.-L. You, A. M. Oleś, and P. Horsch, *Phys. Rev. B* **86**, 094412 (2012).
- [27] M. Kargarian and G. A. Fiete, *Phys. Rev. B* **82**, 085106 (2010).
- [28] L. Fidkowski, *Phys. Rev. Lett.* **104**, 130502 (2010).
- [29] A. M. Turner, Y. Zhang, and A. Vishwanath, *Phys. Rev. B* **82**, 241102 (2010).
- [30] C. Fang, M. J. Gilbert, and B. A. Bernevig, *Phys. Rev. B* **87**, 035119 (2013).
- [31] S. T. Flammia, A. Hamma, T. L. Hughes, and X.-G. Wen, *Phys. Rev. Lett.* **103**, 261601 (2009).
- [32] A. Alexandradinata, T. L. Hughes, and B. A. Bernevig, *Phys. Rev. B* **84**, 195103 (2011).
- [33] F. Kolley, S. Depenbrock, I. P. McCulloch, U. Schollwöck, and V. Alba, *Phys. Rev. B* **88**, 144426 (2013).
- [34] V. Alba, M. Haque, and A. M. Läuchli, *Phys. Rev. Lett.* **110**, 260403 (2013).
- [35] A. M. Läuchli, [arXiv:1303.0741](https://arxiv.org/abs/1303.0741).
- [36] S. M. Giampaolo, S. Montangero, F. Dell'Anno, S. De Siena, and F. Illuminati, *Phys. Rev. B* **88**, 125142 (2013).
- [37] X. Deng and L. Santos, *Phys. Rev. B* **84**, 085138 (2011).
- [38] A. M. Turner, F. Pollmann, and E. Berg, *Phys. Rev. B* **83**, 075102 (2011).
- [39] F. Pollmann and J. E. Moore, *New J. Phys.* **12**, 025006 (2010).
- [40] K. Hasebe and K. Totsuka, *Phys. Rev. B* **87**, 045115 (2013).
- [41] I. H. Kim, *Phys. Rev. B* **87**, 155120 (2013).
- [42] J. Lou, S. Tanaka, H. Katsura, and N. Kawashima, *Phys. Rev. B* **84**, 245128 (2011).
- [43] J. Dubail and N. Read, *Phys. Rev. Lett.* **107**, 157001 (2011).
- [44] H. Yao and X.-L. Qi, *Phys. Rev. Lett.* **105**, 080501 (2010).
- [45] A. J. A. James and R. M. Konik, *Phys. Rev. B* **87**, 241103 (2013).
- [46] M. Pouranvari and K. Yang, *Phys. Rev. B* **88**, 075123 (2013).
- [47] M. Legner and T. Neupert, *Phys. Rev. B* **88**, 115114 (2013).
- [48] I. Pižorn, F. Verstraete, and R. M. Konik, *Phys. Rev. B* **88**, 195102 (2013).
- [49] R. A. Santos, *Phys. Rev. B* **87**, 035141 (2013).
- [50] N. Regnault and B. A. Bernevig, *Phys. Rev. X* **1**, 021014 (2011).
- [51] J. Schliemann, *New J. Phys.* **15**, 053017 (2013).
- [52] N. M. Tubman and D. ChangMo Yang, *Phys. Rev. B* **90**, 081116 (2014).
- [53] X.-L. Qi, H. Katsura, and A. W. W. Ludwig, *Phys. Rev. Lett.* **108**, 196402 (2012).
- [54] A. Chandran, M. Hermanns, N. Regnault, and B. A. Bernevig, *Phys. Rev. B* **84**, 205136 (2011).

- [55] J. Dubail, N. Read, and E.H. Rezayi, *Phys. Rev. B* **86**, 245310 (2012).
- [56] B. Swingle and T. Senthil, *Phys. Rev. B* **86**, 045117 (2012).
- [57] P. Calabrese and A. Lefevre, *Phys. Rev. A* **78**, 032329 (2008).
- [58] A.O. Gogolin, A.A. Nersesyan, and A.M. Tsvelik, *Bosonization and Strongly Correlated Systems* (Cambridge University Press, New York, 1998).
- [59] T. Xiang, *Phys. Rev. B* **53**, R10445 (1996).
- [60] U. Schollwöck, *Rev. Mod. Phys.* **77**, 259 (2005).
- [61] K. Hallberg, *Adv. Phys.* **55**, 477 (2006).
- [62] O. Legeza, R.M. Noack, J. Solyom, and L. Tincani, *Applications of Quantum Information in the Density-Matrix Renormalization Group*, Vol. 739 (Springer, Berlin, 2008).
- [63] M. Führinger, S. Rachel, R. Thomale, M. Greiter, and P. Schmitteckert, *Ann. Phys. (Berlin)* **17**, 922 (2008).
- [64] I. Mondragon-Shem, M. Khan, and T.L. Hughes, *Phys. Rev. Lett.* **110**, 046806 (2013).
- [65] I. Mondragon-Shem and T.L. Hughes, *Phys. Rev. B* **90**, 104204 (2014).
- [66] E.C. Andrade, M. Steudtner, and M. Vojta, *J. Stat. Mech.* (2014) P07022.
- [67] V. Balasubramanian, M.B. McDermott, and M. Van Raamsdonk, *Phys. Rev. D* **86**, 045014 (2012).
- [68] F.D.M. Haldane, *Phys. Rev. Lett.* **60**, 635 (1988).
- [69] B.S. Shastry, *Phys. Rev. Lett.* **60**, 639 (1988).
- [70] M. Greiter, *Mapping of Parent Hamiltonians: from Abelian and non-Abelian Quantum Hall States to Exact Models of Critical Spin Chains* (Springer, New York, 2011).
- [71] R. Thomale, S. Rachel, P. Schmitteckert, and M. Greiter, *Phys. Rev. B* **85**, 195149 (2012).
- [72] A. Chandran, V. Khemani, and S.L. Sondhi, *Phys. Rev. Lett.* **113**, 060501 (2014).
- [73] H. Braganca, E. Mascarenhas, G.I. Luiz, C. Duarte, R.G. Pereira, M.F. Santos, and M.C.O. Aguiar, *Phys. Rev. B* **89**, 235132 (2014).
- [74] M. Levin and X.-G. Wen, *Phys. Rev. Lett.* **96**, 110405 (2006).
- [75] A. Kitaev and J. Preskill, *Phys. Rev. Lett.* **96**, 110404 (2006).
- [76] M. Haque, O. Zozulya, and K. Schoutens, *Phys. Rev. Lett.* **98**, 060401 (2007).
- [77] See Supplemental Material at <http://link.aps.org/supplemental/10.1103/PhysRevLett.113.256404> for bosonic and fermionic representations of the physical Hamiltonian, the effect of certain real-space symmetries on the momentum-space ES, and an analytical proof that the ES deep in the Ising phase for fermions is linear, which includes Ref. [78].
- [78] I. Peschel, *J. Phys. A* **36**, L205 (2003).
- [79] T. Giamarchi, *Quantum Physics in One Dimension* (Oxford University Press, New York, 2013).
- [80] S. Furukawa, M. Sato, S. Onoda, and A. Furusaki, *Phys. Rev. B* **86**, 094417 (2012).
- [81] J. Eisert, M. Cramer, and M.B. Plenio, *Rev. Mod. Phys.* **82**, 277 (2010).
- [82] F. Benatti, R. Floreanini, and U. Marzolino, *Phys. Rev. A* **89**, 032326 (2014).
- [83] F. Benatti, R. Floreanini, and U. Marzolino, *Ann. Phys. (Amsterdam)* **325**, 924 (2010).
- [84] S.-J. Gu, V.M. Pereira, and N.M.R. Peres, *Phys. Rev. B* **66**, 235108 (2002).
- [85] J.C. Bonner and M.E. Fisher, *Phys. Rev.* **135**, A640 (1964).
- [86] <http://www.tacc.utexas.edu>.